ISSN (Print) : 0974-6846
Indian Journal of Science and Technology, *Vol 8(19), DOI:10.17485/ijst/2015/v8i19/61658, August 2015* ISSN (Online) : 0974-5645

Performance Evaluation of Basic Compression Methods for Different Satellite Imagery

Sanjith Sathya Joseph[1*] and Ganesan Ramu[2]

[1]Department of Computer Science and Engineering, Noorul Islam Centre for Higher Education, Kumarcoil, Kanyakumari District - 629 180, Tamilnadu, India; Sanjithss@gmail.com
[2]Department of Electronics and Instrumentation, Noorul Islam Centre for Higher Education,Kumarcoil,Kanyakumari District - 629 180, Tamilnadu, India; dr.ganesh.jass@gmail.com

Abstract

Objective: The purpose of this work is to present the experimental results by comparing the quality of different satellite images LANDSAT 7, MODIS and ASTER after compression, using four different compression methods. **Methods/Analysis:** The satellite images are compressed using four different basic compression methods namely, Pulse code Modulation, Differential Pulse Code Modulation, Discrete Cosine Transform and Sub band Coding. The Compression is performed with three different types of satellite sensor images having different spectral bands, picture bit-rate and level of details using VCDemo software package. **Findings:** The Mean Square Error, Signal to Noise Ratio and Peak Signal to Noise Ratio values are calculated to determine the quality of the images after compression. In order to find the quality of compression methods the Mean Square Error, Signal to Noise Ratio and Peak Signal to Noise Ratio values are collected for different satellite images by compressing with different bitrates. While comparing the obtained values for each compression methods, we found that the compression methods have different impacts in each satellite image according to the bit-rate used for compression and the level of details. **Conclusion:** The study proves that Discrete Cosine Transform and Sub band Coding's performance are worthy for satellite image compression. Where Sub band Coding produces a very good Signal to Noise Ratio and Peak Signal to Noise Ratio values for all bit rates.

Keywords: DCT, Image Compression, MSE, PSNR, Satellite Image Compression, SBC, SNR

1. Introduction

Compression plays a vital role in satellite images because the uncompressed satellite image requires considerable storage capacity and transmission bandwidth[1,30]. Remotely sensed images, which are captured by the satellite sensors, have been widely used in earth observation applications. Hyperspectral imaging sensors can collect an image in which each pixel has the connecting bands of spectra and these large number of spectral channels provide the opportunity for the detailed analysis of the land-cover materials[2], e.g., endmember extraction[3], spectral unmixing[4,5], target detection[6,8], image classification[9,11] and so on. However, as the Hyper Spectral Image (HSI) is intrinsically a data cube which has two spatial dimensions and a spectral dimension, it indicate that the redundancy from both inter-pixel and inter-band correlation is very high and thus the data cube could be high in volume and a compression algorithm should be used in order to reduce the size of the image.

The principles behind compression are most images have a correlation with the neighbouring pixels are generate redundant information. The task of compression is to find less correlated representation of the image. The two fundamental components of compression are redundancy and irrelevancy reduction. Redundancy reduction aims at removing duplication from the signal source. Irrelevancy reduction omits parts of the signal that will not be noticed by the signal receiver, namely the Human Visual System (HVS). In general three types of redundancy can be identified. Spatial redundancy[12], Spectral redundancy[13] and temporal redundancy[14] image compression algorithms aims at reducing the number of bits needed to represent an image by removing the spatial

* *Author for correspondence*

and spectral redundancies as much as possible. For still images temporal redundancy is not needed.

The compression can be classified into two main classes:

- **Lossless vs. Lossy Compression**

In lossless compression scheme, the reconstructed image, after compression is numerically identical to the original image[15,16]. However lossless compression can only achieve a modest amount of compression. The reconstructed using lossy compression contains degradation while relating to the original image. This is because the compression method discards redundant information completely. However, lossy compression methods are capable of achieving much higher compression ratio.

- **Predictive vs. Transform Coding**

In predictive coding information already sent or available is used to predict future values and the differences is coded. Since this is done in the image or spatial domain, it is simple to implement. Differential Pulse Code Modulation (DPCM)[17] is one particular example of predictive coding[18]. Transform coding, transforms the image from its spatial domain representation to a different type of representation using some transform and then codes the transformed coefficients. While comparing to predictive coding transform coding provides better compression ratio[19].

1.1 Images Selected for Analysis

The images selected for analysis are three different satellite sensor images namely LANDSAT, MODIS and ASTER which are shown in Figure 1.

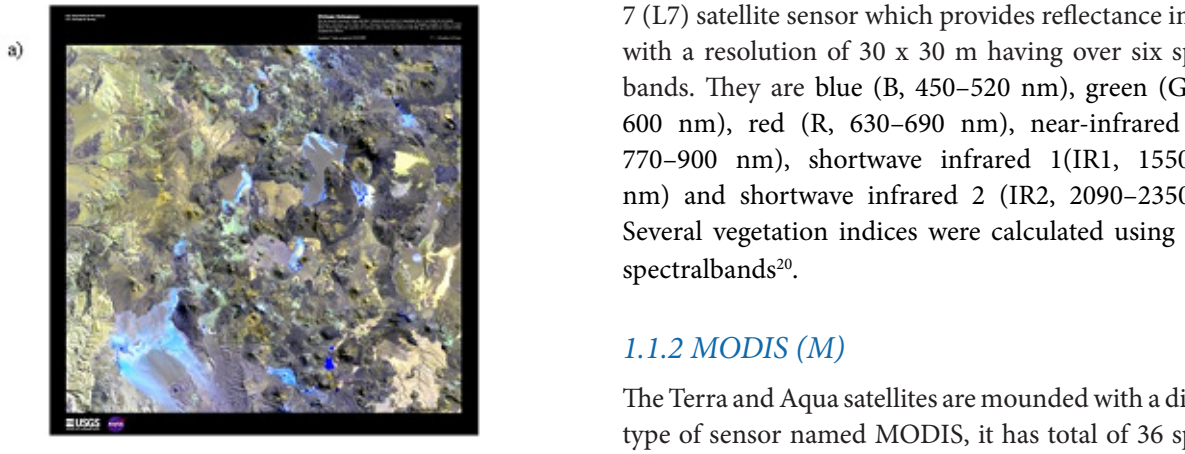

Figure 1. Satellite sensor images a) LANDSAT image b) MODIS image c) ASTER image.

1.1.1 LANDSAT 7 (L)

National Aeronautics and Space Administration Agency (NASA) and US Geological Survey, USA used Landsat 7 (L7) satellite sensor which provides reflectance imagery with a resolution of 30 x 30 m having over six spectral bands. They are blue (B, 450–520 nm), green (G, 520–600 nm), red (R, 630–690 nm), near-infrared (NIR, 770–900 nm), shortwave infrared 1(IR1, 1550–1750 nm) and shortwave infrared 2 (IR2, 2090–2350 nm). Several vegetation indices were calculated using the L7 spectralbands[20].

1.1.2 MODIS (M)

The Terra and Aqua satellites are mounded with a different type of sensor named MODIS, it has total of 36 spectral

bands and its spectral range covers from visible band to thermal infrared bands. It also has the spatial resolution of 250, 500 and 1000 m respectively at the altitude of 2330 km of maximum scan width. The bands from 29 to 36 are the thermal infrared bands (8 – 14 μm) whose spatial resolution is 1000 m and is widely used in the fields of total ozone, cloud layer, cloud height and surface temperature[21].

1.1.3 Advanced Spaceborne Thermal Emission and Reflection Radiometer (ASTER) (A)

The ASTER system has openly available for scholars from past few decades. The system has two main benefits over older LANDSAT satellites, its higher spatial resolution of 15 m and greater overall bandwidth with 14 unique multispectral bands. These bands are fashioned by VINIR (Visible and Near Infrared), SWIR (Short Wave Infrared) and TIR (Thermal Infrared) subsystems. The primary use of ASTER system is to study geological, environmental and population details[22].

1.2 Compression Methods Used

1.2.1 Pulse Code Modulation (PCM)

The most common method used for digital television encoding signals is the linear Pulse Code Modulation (PCM). In order to storage and transmission of the digitized television signal it is need to reduce the number of bits on the encoded signal as much as possible without deleting to much of relevant information, for implementing this task PCM and DPCM is well-known[23].

In PCM system the incoming signal is sampled and the amplitude of each sample is measured with a fixed scale. The distinct levels on the scale can have a linear or a nonlinear distribution and they are numbered in order, starting with a fixed zero–level. The amplitude of each sample is digitized by rounding off its amplitude to the nearest distinct scale level and assigning the appertaining number to the sample. These numbers can be processed or transmitted and each number is easily reconverted in the PCM decoder.

1.2.2 Differential Pulse Code Modulation (DPCM)

The DPCM compression module implements a spatially predictive compression scheme.

The amplitude of the incoming sample is measured with a sliding scale and the zero level of the scale is put at the quantized amplitude of the previous sample and the distinct levels on the scale are again numbered in order. Amplitude of each sample is measured with respect to the previous sample and the resulting numbers shows the successive samples[23].

1.2.3 Sub Band Coding (SBC)

The SBC compression module implements SBC coder with global bit allocation. Different subband decompositions can be selected and different QMF filters can be selected. Multiple subbands are obtained by tree structured subband decompositions. The subbands are quantized based on a user-selectable PDF model. The quantizer representation levels are entropy encoded[24].

In the case of M subbands of equal bandwidth each subband has been subsampled by sqrt(M) in each dimension. If Bk bits are assigned to subband k, we get the average bitrate as,

$$B = \frac{1}{M}\sum_{k=1}^{M} B_k$$

Here k represents the subbands ij of the previous section indexed in some convenient order.

1.2.4 Discrete Cosine Transform (DCT)

The Discrete Cosine Transform (DCT) receives an N x N block matrix image, which is separate into small image blocks (4x4, 8x8, 16x16…) in which each block is transformed from the spatial domain to the frequency domain. DCT decomposes signal into spatial frequency components called DCT coefficients[25, 26]. The lower frequency DCT coefficients appear towards the first line/ first column of the DCT matrix and the higher frequency coefficients are in the last line or in the last column of the DCT matrix. The quantization is used to discard insignificant data without introducing any artifacts to the image. After quantization, the majority of the DCT coefficients are equal to zero[27].

1.3 VCDemo Software

The VCDemo is an image and video compression learning tool which is a fully menu-driven package developed by Delft University of Technology Faculty of Electrical Engineering, mathematics and Computer Science and Department of Intelligent Systems, Netherland. It is operated by selecting compression techniques and parameters using buttons

VCDemo is a tool assisting the learning process, but does in itself not explain the compression techniques. The

VCDemo software can be freely downloaded from http://ict.ewi.tudelft.nl/vcdemo.

2. Materials and Methods

In this study satellite images taken by three different types of sensors (M, L, A) serve as the data source. These three sensors has different spectral bands and different imaging resolution. The uncompressed satellite images are available from the following web page http://erous.usgs.gov/imagegallery is used in this analysis. These images are in tiff file format with a resolution of 7904 x 8512 and file size of 192 MB. The obtained images are resized into a resolution of 1024 x 1024 and used as the input file for VCDemo v 5.03 available at http://www-sipl.technion.ac.il/Info/Downloads_VCDemo_e.shtml.

2.1 Image Quality Assessment

The quality of a compressed image is evaluated in order to measure the degradation in digital images while lossy compression is performed and to find how the image quality is affected by the compression method[16]. The image quality are evaluated by MSE, SNR and PSNR. MSE is the cumulative square error if the error is minimum. MSE values will be less and it translates to a higher value of PSNR. SNR is the ratio between the meaningful information and the unwanted information. It is a measure of the signal strength related to background noise.

PSNR is a measure of peak error between the compressed image and original image. PSNR value should be higher for better compression, signal is the original image and noise is the error in the reconstructed image.

The evaluation process is done based on the design of the elements in input and output matrix. By this method, the quality of the different compression method is performed and also comparison of the results using different compression ratio is done.

Matrix a is denoted as the input of compression system with elements a_{ij}, with i, j, where M denotes the number of image elements in vertical path and N denotes the number of image elements in horizontal path. MxN is the total number of image elements[28].

The output matrix created by the compression system is A' with elements a'_{ij}. The error or the loss of image quality is measured by the distance between the elements of matrices A and A'. Normally the error will be larger in higher compression ratios. The compression ratio can be set by the user, which directly influence in the data size of the compressed image[28].

The total reconstruction error is defined as:

$$E = \sum_{i=0}^{m-1}\sum_{j=0}^{n-1}\left\|a_{ij} - a'_{ij}\right\|^2$$

The distance between matrices A and A' is frequently calculated using the MSE:

$$MSE = \frac{E}{MN} = \frac{1}{MN}\sum_{i=0}^{m-1}\sum_{j=0}^{n-1}\left\|a_{ij} - a'_{ij}\right\|^2$$

$$SNR = 20 * \log_{10}\left(\frac{Psignal}{Pnoise}\right)$$

The total number of pixels in image is MxN and the sum will be applied to all image elements. The amplitude of image elements are in the range [0, 2n-1], n is the number of bits needed for binary representation of amplitude of each element in the original image. MSE considers only the difference between amplitudes, so PSNR is introduced in order to consider amplitudes of image elements.

$$PSNR = 10.\log_{10}\left(\frac{MAX_I^2}{MSE}\right) = 20.\log_{10}\left(\frac{MAX_I}{\sqrt{MSE}}\right)$$

The MAX_I is the variable which represents maximum amplitude value of image pixel. When the amplitude of the image pixel is represented by B bits, MAX_I is 2B -1. We can define n = 8 bits/image element by:

$$PSNR = 10.\log_{10}\left(\frac{255^2}{MSE}\right)$$

PSNR values for classic "lossy" compression images will be between 30 to 50 dB.

In order to find the quality of the reconstructed images the compression is performed using VCDemo package compression modules, six different bit-rates are used 1, 2, 3, 4, 5 and 6bpp. For all the three images the difference between the original and reconstructed images are calculated with Mean Square Error (MSE), Signal to Noise Ratio (SNR) and Peak Signal to Noise Ratio (PSNR). The values obtained for the images are given in the Tables 1, 2, 3 and 4 respectively.

Table 1. MSE, SNR and PSNR values For PCM compression method

Bitrate (bpp)	MSE			SNR (dB)			PSNR (dB)		
	L	M	A	L	M	A	L	M	A
1	2034.0	1847.0	1846.0	3.6	3.7	2.8	15.0	15.5	15.5
2	481.2	493.0	443.7	9.9	9.4	9.0	21.3	21.2	21.7
3	119.9	122.6	117.0	15.9	15.4	14.8	27.3	27.2	27.4
4	30.0	30.5	30.4	21.9	21.5	20.6	33.4	33.4	33.3

Table 2. MSE, SNR and PSNR values for DPCM compression method

Bitrate	MSE			SNR (dB)			PSNR (dB)		
(bpp)	L	M	A	L	M	A	L	M	A
1	348.2	383.9	411.0	11.3	10.5	9.3	22.7	22.3	22.0
2	103.4	107.3	109.4	16.5	16.0	15.1	28.0	27.0	27.7
3	36.7	36.7	31.9	21.0	20.7	20.4	32.5	32.5	33.1
4	13.1	12.5	9.3	25.5	25.4	25.8	37.0	37.2	38.5

Table 3. MSE, SNR and PSNR values for DCT compression method

Bitrate	MSE			SNR (dB)			PSNR (dB)		
(bpp)	L	M	A	L	M	A	L	M	A
1	81.5	69.6	116.9	17.6	17.9	14.8	29.0	29.7	29.5
2	30.3	19.1	30.3	20.6	23.5	20.6	33.3	35.3	33.3
3	7.2	4.8	7.2	26.9	29.5	26.9	39.5	41.3	39.5
4	2.5	1.9	2.5	31.5	33.5	31.5	44.2	45.3	44.2

Table 4. MSE, SNR and PSNR values for SBC compression method

Bitrate	MSE			SNR (dB)			PSNR (dB)		
(bpp)	L	M	A	L	M	A	L	M	A
1	82.3	67.6	110.9	17.5	18.0	15.0	29.0	29.8	27.7
2	29.4	17.1	29.4	20.8	24.0	20.8	33.4	35.8	33.4
3	6.4	4.1	6.4	27.4	30.2	27.4	40.1	42.0	40.1
4	1.9	1.3	1.9	32.6	35.2	32.6	45.3	47.0	45.3

3. Result and Discussion

The MSE, SNR and PSNR values are calculated for all images using the four compression methods are depicted in the Tables 1, 2, 3 and 4.

It was observed from the investigational results that as the bit rates are increased the values of MSE decreases for all the compression methods. For lower Bitrate (bpp) MSE values are gradually higher and vice versa.

Tables 1 and 2 shows the values obtained by the PCM and DPCM compression methods the PCM compression method gains very high MSE values for all the three image types while using Bitrate 1, where DPCM achieved a nominal values. For Bitrates 2 to 4 PCM yields higher MSE values than DPCM. While considering SNR and PSNR values DPCM has gained higher values than PCM.

Table 3 and Table 4 depicts the values attained by DCT and SBC compression methods for all the images the higher MSE values are obtained by DCT and SBC yields good SNR and PSNR values for all image types in different Bitrates.

A Compressed image is a better image if it has lower MSE and higher PSNR. It also seems that for higher rate of compression the noise in the image increases i.e. lower value of SNR and PSNR[29]. The MSE values acquired by the three satellite sensor images using different compression methods is displayed in Figure 2, while analysing the graphs all the four compression method yields lesser MSE value for all images while applying Bitrate 4. PCM gains very high MSE values for all three images DPCM gains higher MSE values for all images and lower than PCM but higher than DCT. SBC produces almost similar values like DCT.

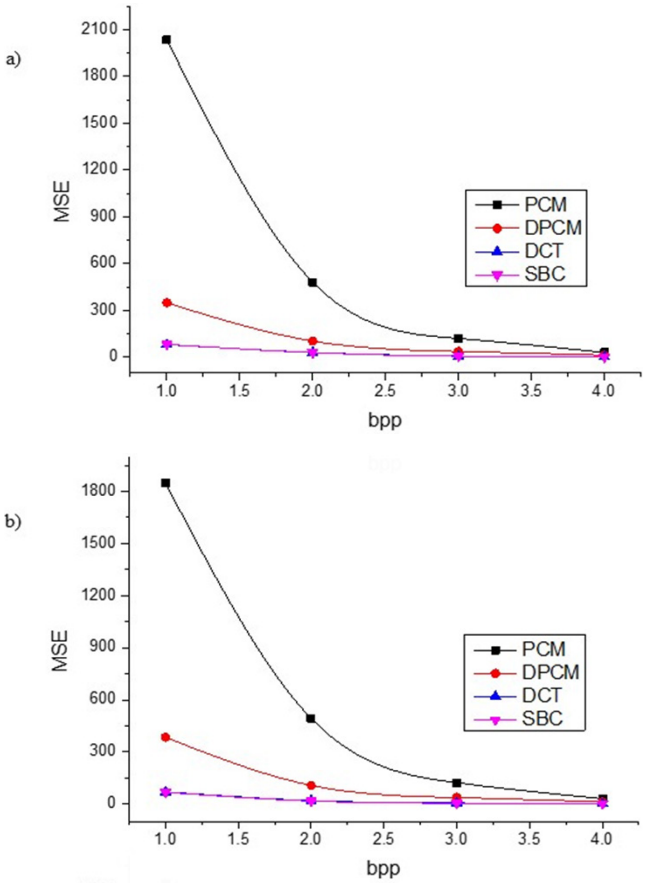

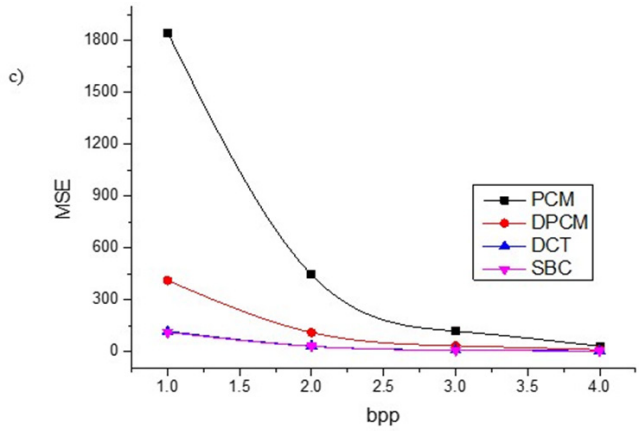

Figure 2. MSE values obtained by different compression methods for a) LANDSAT Image, b) MODIS Image, c) ASTER Image.

SNR values attained by the compression methods are plotted in Figure 3, PCM obtained very low SNR values than DPCM for all Bitrates, DCT and SBC had gained almost same SNR values but for higher Bitrates SBC yields higher SNR values.

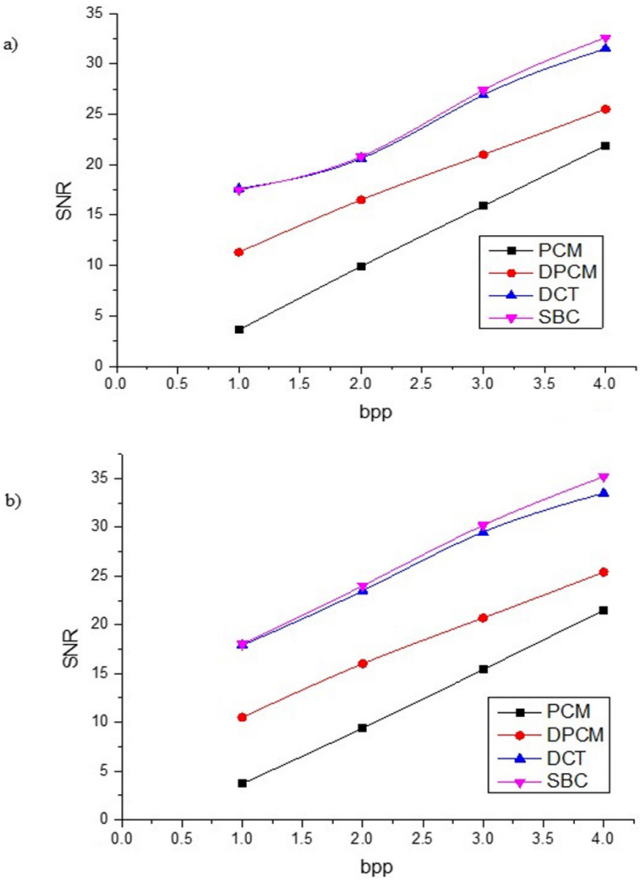

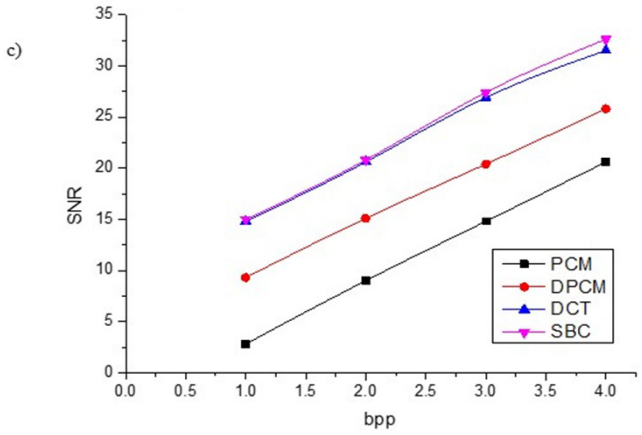

Figure 3. SNR values obtained by different compression methods for a) LANDSAT image, b) MODIS image, c) ASTER image.

PSNR values for all compression method is displayed in Figure 4, PCM obtained very low PSNR values than DPCM for all Bitrates, DCT and SBC had gained almost same PSNR values but for higher Bitrates SBC yields higher PSNR values. While comparing all the four compression methods DCT and SBC can perform well in compressing satellite imagery, but SBC can yield better values than DCT.

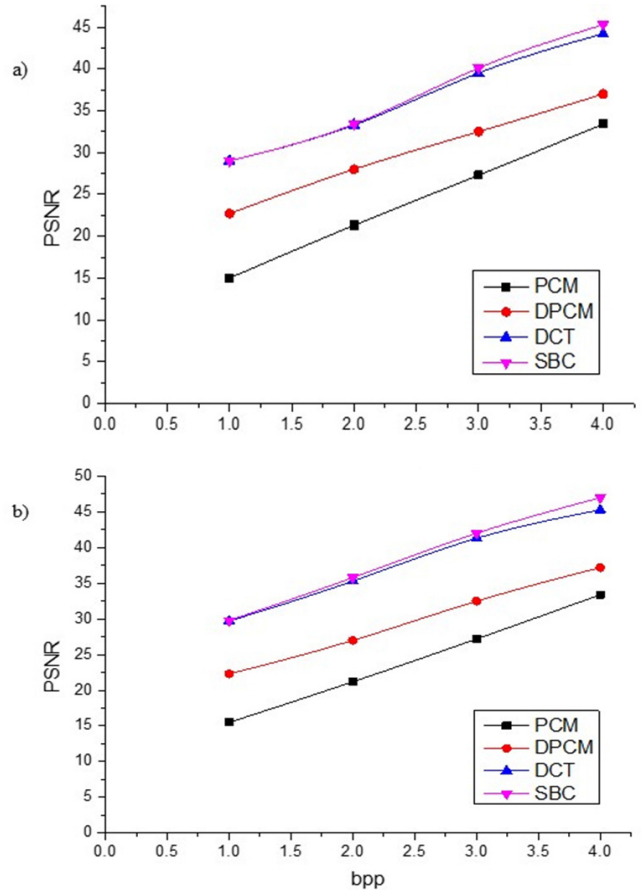

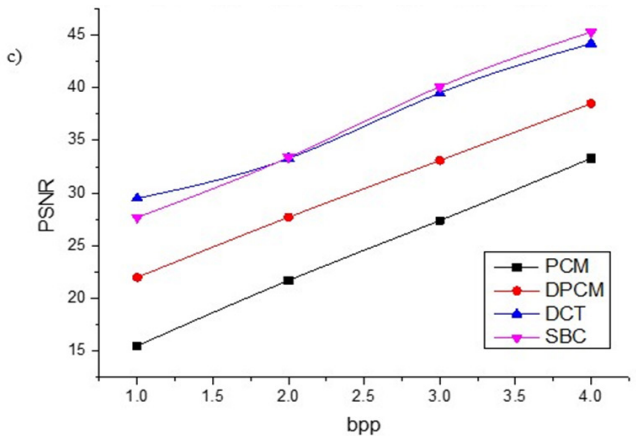

Figure 4. PSNR values obtained by different compression methods for a) LANDSAT image, b) MODIS image, c) ASTER image.

4. Conclusion

In this work three satellite sensor images namely LANDSAT, MODIS and ASTER are chosen and compressed using different basic compression methods and their MSE, SNR and PSNR values have been obtained in order to analyse the quality of image after compression. The impact of image details plays an important role in satellite image compression since the three images are different sensor image and have different image details. Finally DCT and SBC have good result in satellite image compression. The SNR and PSNR values yield by SBC is good for even higher and lower bit rates.

The PCM compression method provides poorest result compared to other three compression methods. These methods produce low SNR and PSNR values for all three image types, where DPCM compression produces somewhat better result than PCM.

All the four compression methods produces higher MSE values for higher bit rates. The SNR and PSNR values increase while the bit rate values increases for all the compression methods.

DCT and SBC produces almost same MSE values for all bit rates, the SNR and PSNR values produced for higher bit rates for all the three images have slight variations.

According to the analysis PCM and DPCM yields worst results where as DCT and SBC are good satellite imagery compression. According to the values obtained for the LANDSAT, MODIS and ASTER images SBC produces a very good SNR and PSNR values for all bit rates.

5. References

1. Sanjith S, Ganesan R. Control, instrumentation, communication and computational technologies (ICCICCT). International Conference; Kanyakumari, India. 2014 July 10-11. p. 1159–63.
2. Plaza A, Benediktsson JA, Boardman JW, Brazile J, Bruzzone L, Camps-Valls G, Chanussot J, et al. Recent advances in techniques for hyperspectral image processing. Remote Sensing of Environment. 2009 Sep; 113(S1):S110–22.
3. Zhang B, Sun X, Gao L, Yang L. Endmember extraction of hyperspectral remote sensing images based on the ant colony optimization (ACO) algorithm. IEEE Transactions on Geoscience and Remote Sensing. 2011 Jul; 49(7):2635–46.
4. Zhang B, Gao J, Gao L, Sun X. Improvements in the ant colony optimization algorithm for endmember extraction from hyperspectral images. Selected Topics in Applied Earth Observations and Remote Sensing. IEEE Journal. 2013 Apr; 6(2):522–30.
5. Bioucas-Dias JM, Plaza A, Camps-Valls G, Scheunders P, Nasrabadi NM, Chanussot J. Hyperspectral remote sensing data analysis and future challenges. IEEE Geoscience and Remote Sensing Magazine. 2013 Jun; 1(2):6–36.
6. Lu X, Wu H, Yuan Y, Yan P, Li X. Manifold regularized sparse NMF for hyperspectral unmixing. IEEE Transactions on Geoscience and Remote Sensing. 2013 May; 51(5):2815–26.
7. Du B, Zhang L, Tao D, Zhang D. Unsupervised transfer learning for target detection from hyperspectral images. Neurocomputing. 2013 Nov; 120:72–82.
8. Du B, Zhang L. Target detection based on a dynamic subspace. Pattern Recognition. 2014 Jan; 47(1):344–58.
9. Zhang L, Zhang L, Tao D, Huang X. Sparse transfer manifold embedding for hyperspectral target detection. IEEE Transactions on Geoscience and Remote Sensing. 2014 Feb; 52(2):1030–43.
10. Li W, Tramel EW, Prasad S, Fowler JE. Nearest regularized subspace for hyperspectral classification. IEEE Transactions Geoscience and Remote Sensing. 2014 Jan; 52(1):477–89.
11. Kang X, Li S, Benediktsson JA. Spectral–spatial hyperspectral image classification with edge-preserving filtering. IEEE Transactions on Geoscience and Remote Sensing. 2014 May; 52(5):2666–77.
12. Zhang L, Zhang L, Tao D, Huang X. On combining multiple features for hyperspectral remote sensing image classification. IEEE Transactions on Geoscience and Remote Sensing. 2012 Mar; 50(3):879–93.
13. Le Gall DJ. The MPEG video compression algorithm. Signal Processing: Image Communication. 1992 Apr; 4(2):129–40.
14. Brunello D, et al. Lossless compression of video using temporal information. IEEE Transactions on Image Processing. 2003 Feb; 12(2):132–9.
15. Le Gall D. MPEG: a video compression standard for multimedia applications. Communications of the ACM. 1991; 34(4):46–58.
16. Said A., Pearlman WA. An image multiresolution representation for lossless and lossy compression. IEEE Transactions on Image Processing. 1996 Sep; 5(9):1303–10.

17. Burt PJ, Adelson EH. The Laplacian pyramid as a compact image code. IEEE Transactions on Communications. 1983 Apr; 31(4):532–40.
18. Habibi A., Hershel R. A unified representation of differential pulse-code modulation (DPCM) and transform coding systems. IEEE Transactions on Communications. 1974 May; 22(5):692–6.
19. De Vore RA, Jawerth B, Lucier BJ. Image compression through wavelet transform coding. IEEE Transactions on Information Theory. 1992 Mar; 38(2):719–46.
20. Scudiero ES, Skaggs TH, Corwin DL. Regional Scale Soil Salinity Evaluation Using Landsat 7, Western San Joaquin Valley, California, USA. Geoderma Regional. 2014 Nov-Dec; 2-3:82–90.
21. Sanjith S, Ganesan R, Isaac RS. Experimental analysis of compacted satellite image quality using different compression methods. Advanced Science, Engineering and Medicine. 2015 Mar; 7(3):227–33.
22. Bhadra BK, Pathak S, Karunakar G, Sharma JR. ASTER data analysis for mineral potential mapping around Sawar-Malpura area, Central Rajasthan. Journal of the Indian Society of Remote Sensing. 2013 Jun; 41(2):391–404.
23. Van Buul M. Hybrid D-PCM, a combination of PCM and DPCM. IEEE Transactions on Communications. 1978 Mar; 26(3):362–8.
24. Woods JW, O'neil SD. Subband coding of images. IEEE Transactions on Acoustics, Speech and Signal Processing. 1986 Oct; 34(5):1278–88.
25. Richardson IE. Video codec design: developing image and video compression systems. John Wiley & Sons; 2002 Jun.
26. Agostini VL, Silva IS, Bampi S. Pipelined fast 2D DCT architecture for JPEG image compression. 14th Symposium on IEEE Integrated Circuits and Systems Design; Pirenopolis. 2001. p. 226–31.
27. Watso AB. DCT quantization matrices visually optimized for individual images. IS&T/SPIE's Symposium on Electronic Imaging: Science and Technology. International Society for Optics and Photonics; 1993 Sep.
28. Ilic S, Petrovic M, Jaksic B, Spalevic P, Lazic L, Milosevic M. Experimental analysis of picture quality after compression by different methods. Przegląd Elektrotechniczny. 2013; 89(11):190–4. ISSN 0033-2097.
29. Al-Najjar AYY, Soong DC. Comparison of image quality assessment: PSNR, HVS, SSIM, UIQI. International Journal of Scientific & Engineering Research. 2012 Aug; 3(8). ISSN: 2229-5518.
30. Ganesan P, Rajini V, Sathish BS, Kalist V, Khamar Basha SK. Satellite Image Segmentation Based on YCbCr Color Space. Indian Journal of Science and Technology. 2015 Jan; 8(1):35–41.